

Research and Development Status of Microwave Discharge Ion Thruster $\mu 20$

IEPC-2005-055

Presented at the 29th International Electric Propulsion Conference, Princeton University,
October 31 – November 4, 2005

Kazutaka Nishiyama,^{*} Yukio Shimizu[†] and Hitoshi Kuninaka[‡]
Japan Aerospace Exploration Agency / Institute of Space and Astronautical Science,
Sagamihara, Kanagawa, 229-8510, Japan

Takashi Miyamoto[§]
Kyushu University, Higashi-ku, Fukuoka, 812-8581, Japan

Miho Fukuda^{**}
Hosei University, Koganei, Tokyo, 184-8584, Japan

and

Tatsuya Nakai^{††}
The University of Tokyo, Bunkyo-ku, Tokyo, 113-8656, Japan

Abstract: Japan's HAYABUSA asteroid explorer, launched on May 9 2003, has executed the orbit maneuver using microwave discharge ion engines " $\mu 10$," which have electro-static grids of effective diameter 10cm and established 25,800 hours the total numbers of space operational time to generate 1,400m/s delta-V with 22kg xenon propellant. The ion engines accomplished two-thirds of the orbit maneuver in the round-trip space mission. In order to adapt to a wide variety of the space flights as well as advance the technology of the ion engine, the " $\mu 20$ " is under research and development. The " $\mu 20$ " has a 20cm diameter grid and aims to achieve 30mN/kW thrust power ratio. The ion source with a microwave antenna can generate 500mA ion current consuming 100W 4.25GHz microwave power. The 20cm diameter grid assembly made of a high stiffness carbon-carbon composite material was machined and passed the vibration test. Magnetic field and propellant injection method of the ion source has been optimized. The performance is highly dependent on the propellant injection method. The same neutralizer as $\mu 10$ can be used more efficiently with small addition of propellant and microwave power.

* Research Associate, Space Transportation Division, nishiyama@ep.isas.jaxa.jp.

† Research Engineer, Space Transportation Division, shimizu@isas.jaxa.jp.

‡ Professor, Space Transportation Division, kuninaka@isas.jaxa.jp

§ Graduate Student, Interdisciplinary Graduate School of Engineering Sciences, miyamoto@ep.isas.jaxa.jp.

** Graduate Student, Department of Mechanical Engineering, fukuda@ep.isas.jaxa.jp.

†† Graduate Student, Department of Aeronautics and Astronautics, nakai@ep.isas.jaxa.jp.

I. Introduction

In order to advance the technology of the cathode-less microwave discharge ion engine “ μ ” family we are executing two developing program: $\mu 20$ and $\mu 10\text{Hisp}$. The former is a 20cm diameter microwave discharge ion engine. The latter is a higher specific impulse version of $\mu 10$. The target of R&D on $\mu 20$ is to achieve 30mN/kW in the thrust power ratio. The $\mu 10$ system generates a 140mA ion beam with 32W microwave power so that the ion production cost is 230eV, which is average in 10cm-class ion source. However, the conversion efficiency of the microwave generator is not good so that the total efficiency and the thrust power ratio are inferior to those of the electron bombardment type ion thrusters. The $\mu 20$ system aims to generate ions at less than 200eV ion production cost. And optimized design on the microwave network will achieve the target thrust power ratio. The highly biased ion source of the electron bombardment ion thruster is fed power, command and telemetry through isolation transformers and/or optical equipments, which are nervous and weighty components. The μ technology eliminates these isolations because the ion source includes no active electronics devices as illustrated in Figure 1. Whereas, the DC block as a microwave damming up DC voltage, is very important. Table 1 summarizes the performance of the three models.

In this paper research and development status of $\mu 20$ updated after the last report¹, especially the results of extensive beam extraction test for various propellant injection methods will be presented.

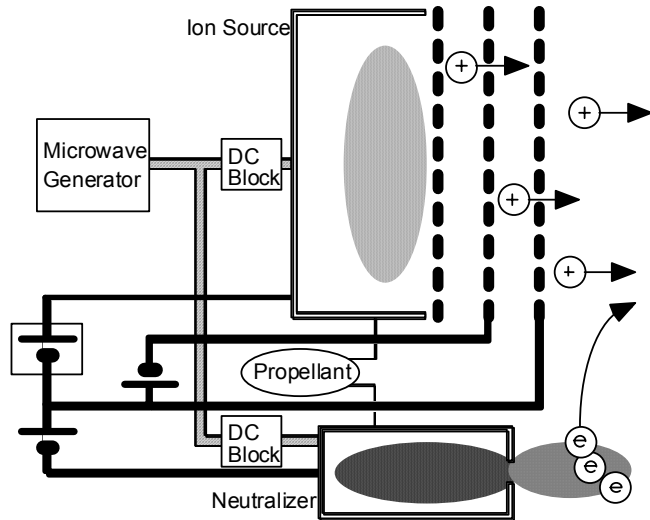


Figure 1. System configuration of microwave discharge ion thruster.

Table 1. Performance of “ μ ” series ion thrusters.

Items	$\mu 10$ (achieved)	$\mu 20$ (target)	$\mu 10\text{Hisp}$ (target)
Ion Prod. Cost	230eV	200eV	230eV
Beam Current	140mA	500mA	140mA
μw Power	32W	100W	32W
Screen Voltage	1,500V	1,200V	15,000V
Specific Imp.	3,000sec	2,800sec	10,000sec
Thrust	8.5mN	27mN	27mN
System Power	350W	900W	2,500W
Thrust/Power	22mN/kW	30mN/kW	11mN/kW

II. Ion Source

An ECR discharge was first applied to a 30-cm plasma generator for ion propulsion by H. Goede at the TRW Space and Technology Group in the late 1980's². A few years after, this research was ceased, and we at the ISAS electric propulsion section started work on a 10-cm ion thruster using the same plasma discharge mechanism. Goede introduced the advantages of having an azimuthal cusp (so called ring-cusp) magnetic field arrangement, in contrast to the axial-line cusp. Accordingly, we followed his proposal and designed initial laboratory models just by scaling down his device. However, it turned out that the ring-cusp configuration in a bucket-like discharge chamber with large volume³ was not suitable for a 10-cm plasma generator, and it was found during development process of $\mu 10$ by ISAS⁴ that a magnet system with a pair of magnet lines inclined to the plasma source exit and a much shorter chamber length⁵ yields higher performance. Incidentally, the $\mu 10$ ion source has a very short plasma chamber in which the ion optics is located very close to the ECR region corresponding to a magnetic field strength of 0.15 T⁶. In the course of developing the $\mu 20$ ion source, we have considered several chamber designs as summarized in the previous report⁷. After the performance evaluation tests of these plasma generators using a punching metal as an ion collector, the magnetic field and microwave launcher design that will be described hereafter were selected and further performance tuning has been conducted under beam extraction using ion optics.

A. Magnetic Field Design

The magnetic field and magnet arrangement are illustrated in Figure 2 and Figure 4. The distance between the magnet lines is basically similar to the distance value for the $\mu 10$. The only salient difference is the most inner magnet lines, where the distance to the neighboring magnet line is twice the distance for others; this way, microwave propagation to the outer ECR regions is not disturbed by the production of a plasma being too dense around the inner ECR regions. This has two magnet bridges between “2N” and “4N” rows shown in Figure 4 in the radial directions so that high energy electrons can fly between inner and outer discharge regions by $E \times B$ drift or grad B ($B \times \nabla B$) drift. With this magnet arrangement, two crescent shaped plasma rings were produced at the same time.

Because the ECR plasma is tightly confined in the banana-shaped region between the magnetic field cusps, the ion optics positioned far from the ECR region cannot extract the produced ions efficiently. If the ion optics are located too close to the ECR region, the plasma production volume decreases due to obscuration by a screen grid and electrons that pass through the ECR zone more than once may be lost to the grid surface, resulting in an increase in the ion production cost. Thus, the discharge chamber axial length is one of the main design parameters. The axial length of 30mm is the best value we obtained so far.

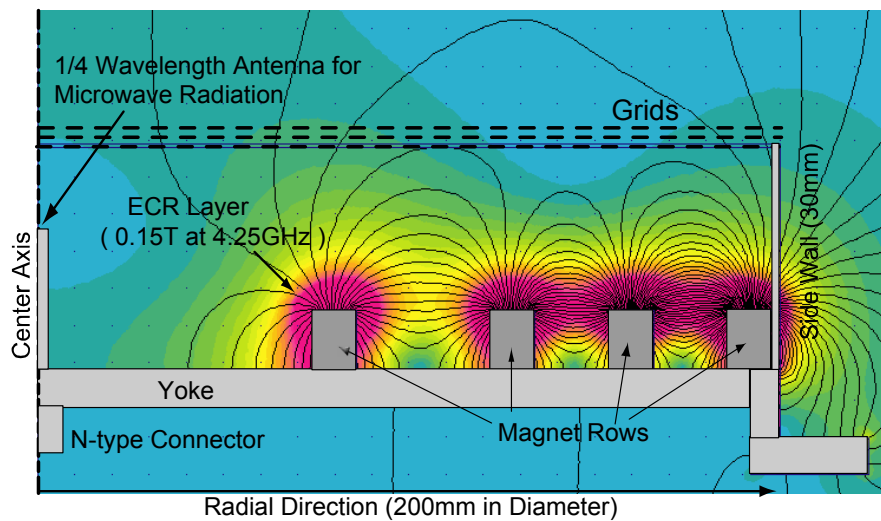


Figure 2. Magnetic field inside the discharge chamber of the ion source.

B. Microwave Launcher

The R&D of $\mu 20$ started by utilizing a coaxial-line to circular-waveguide transducer, which is inherited from $\mu 10$ ion thruster. Original laboratory models of the $\mu 10$ employed a waveguide-based microwave transmission system, as is typical in ground applications of ECR plasma sources. Since building the entire microwave circuit using waveguides is impossible due to the weight penalty it imposes, a microwave amplifier output is connected to the ion source via coaxial cables in case of space applications. Although this microwave launcher is sufficiently optimized and its optimization process is well established, its overall length being too long and its relatively large weight recommend switching to a better microwave launching method. The current $\mu 20$ configuration shown in Figure 2 employs a microwave excitation probe (or antenna) at the center of the discharge chamber. This direct probe insertion has been employed in our neutralizer by using an SMA type connector. Considering that, as an ion source the microwave power input is much larger than that of the neutralizer, high power connectors are desirable, such as N- and TNC-type. Experiments were conducted using a commercial N-type feed-through whose center conductor was modified so that it works as a quarter-wavelength monopole antenna. The $\mu 20$ has no microwave impedance matching component. Thus the reverse power sometimes exceeds 20W. In this paper “net microwave power” at the antenna connector was calculated by taking the reflected power and cable loss into account. But the ion production costs were calculated by adding the reflected power into discharge loss. Efficiency of microwave amplifier was not taken into account.

C. Grid Assembly⁸

In order to adapt a two times larger grid assembly a high stiffness carbon-carbon composite material is desirable. Several candidate materials were tested on the basic physical properties: the flexural strength, the flexural modulus, tensile strength, tensile elastic modulus, Poisson's ratio, remaining strain, electric resistivity, thermal emissivity, thermal diffusivity, thermal expansion, so on. The key parameter is the tensile elastic modulus. The new material has about three times higher Young's modulus than that of $\mu 10$ grid material. Before manufacturing the grid system, the MSC/NASTRAN program has been applied to the structural analysis using 33,000 numbers of nodes and about 46,500 numbers of elements. It showed the lowest characteristic frequency 150Hz out of plane, which is allowable for the rocket launch environment. The analytical result of the primary vibration mode and an emphatic displacement revealed that a 250Grms vibration input causes 0.7MPa stress in the grid, which is positive in the margin of safety. Based on the analysis the 20cm diameter grid system was machined shown in Figure 3. Grid thicknesses are 0.95 mm for the screen grid 1.0 mm for both the accelerator grid and decelerator grid. Grid separations are 0.7 mm between screen and accelerator and 0.20 mm between accelerator and decelerator, respectively. The screen-accelerator gap decreases as the operating temperature increases due to thermal expansion of the grids support ring. After the initial beam extraction test, it was devoted to a set of random vibration tests in 3-axes of 10 Grms in all directions. Because these grids are flat type, grids hit each other during vibration tests. However, neither apparent damage or performance degradation were found after the tests and they were accepted. All the experimental result in this paper were obtained with this optics after the vibration tests. Another screen grid of 0.75mm thickness has just been fabricated and will be evaluated very soon.

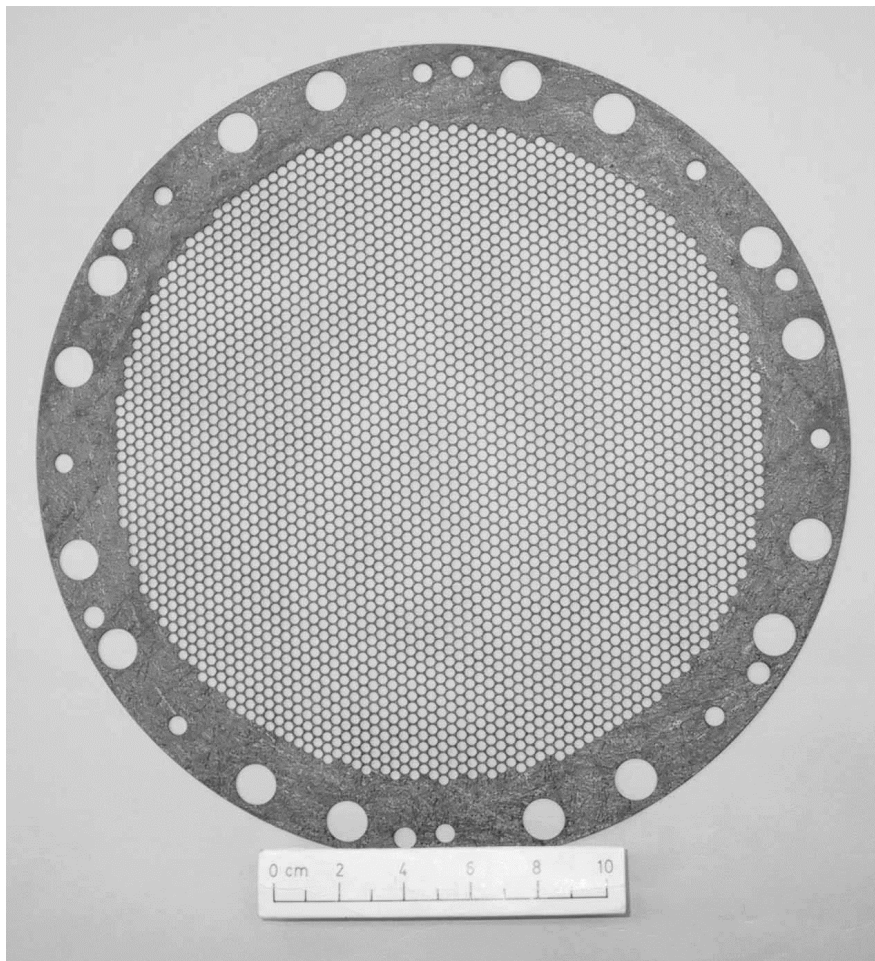


Figure 3. 20cm diameter grid.

D. Propellant Injectors

We have recognized the importance of propellant injection method from the beginning of the $\mu 20$ development⁹. The initial work was conducted by using a punching metal for ion current collection. In such configurations, a large number of ions are reflected back from the collector surface after losing their positive charge. Thus the situation as for neutral particle flow inside the discharge chamber is quite different from the case where beam ions are extracted by ion optics, even if the averaged discharge pressures in both cases are maintained the same. We carried out extensive tests changing the propellant injector configurations under beam extraction.

Figure 4 shows the some of gas ports on the yoke (end plate) and their combinations used in the tests. Although more than 10 patterns have been evaluated, only remarkable results will be shown herein. All the ports are cylinders 5mm in diameter and 5mm in length. The propellant was injected to downstream direction in parallel to the thruster center axis. The total mass flow rate of xenon was controlled with one controller and the propellant feeders were evenly divided before being connected to the ports, but the exact distribution ratios were not measured. There are several valves in feed lines so that the gas distribution pattern can be quickly and dynamically changed with keeping the thruster operating. The vacuum pressures near the thruster in the test facility were 6.0×10^{-5} Pa without load and 1.0×10^{-3} Pa with 10sccm xenon flow, respectively. The beam extraction was carried out with a screen voltage of 1200V, an accelerator voltage of -350 V and a decelerator voltage of 0V. A 2% thoriated tungsten filament was used as a neutralizer.

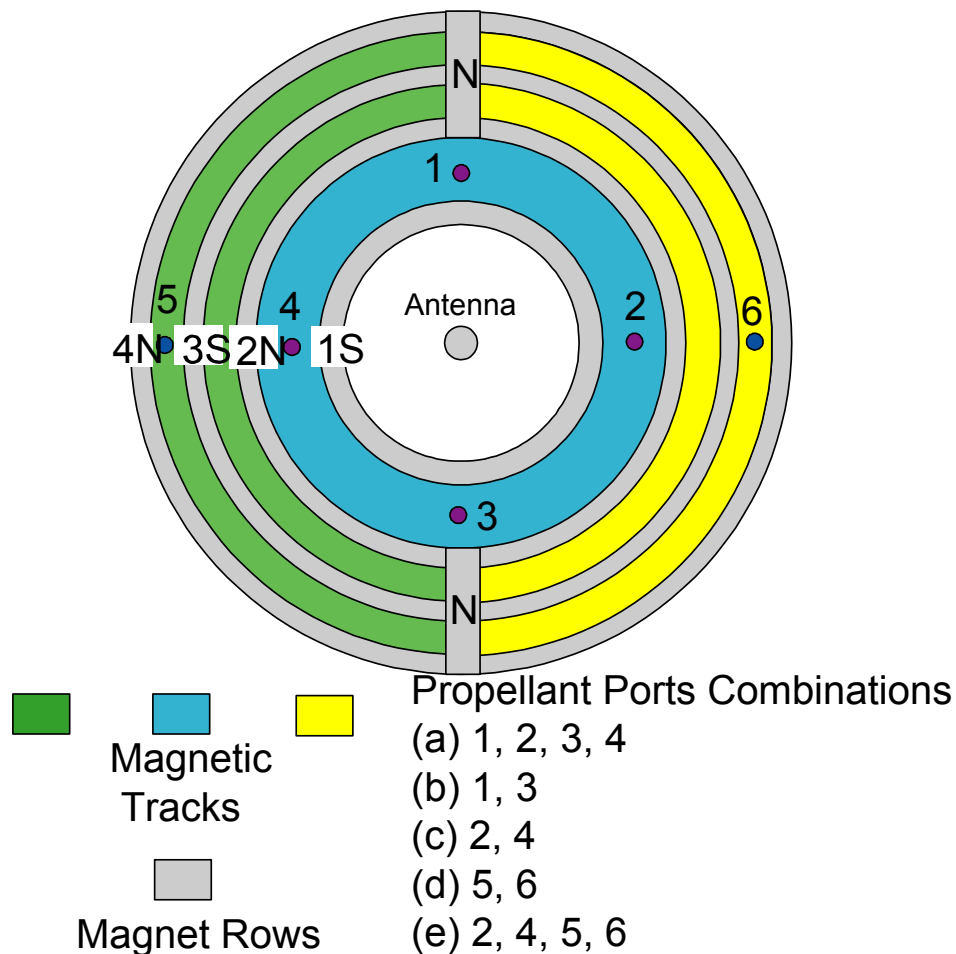


Figure 4. Layout of magnets and propellant ports.

Figure 5 shows ion beam currents as a function of net microwave power for various kinds of gas injection configurations. Ion beam currents for three xenon flow rates are shown in each plot. Photographs of discharge plasma are also shown. Luminous spots in the photos correspond to the locations of gas ports. The sequential characters (a)~(e) in Figure 5 indicate the same port combinations depicted in Figure 4.

Figure 5-(a) shows the worst performance case that we have investigated so far. Although the beam currents gradually increase as the flow rates increase, the current is very small as if it was generated by a relatively smaller thruster. The contribution of ion beam production at outer magnetic tracks (green and yellow zones in Figure 4) is probably small. The case where the four ports locations were rotated by 45° from Figure 5-(a) positions showed 7% larger beam current.

Just removing two ports (No.2 and No.4 in Figure 4) from the configuration (a) drastically improves the performance as shown in Figure 5-(b). This difference is a typical case that suggests there is an optimum number of gas ports per plasma ring. It seems that uniform gas feed by large number of injectors like gas distributors of other ion thrusters is not necessarily advantageous in the microwave discharge types.

The two ports configuration (c) in different phase angle position than (b) indicates better performance than (a), but is worse than the case (b). The beam currents are larger in the smaller flow rate conditions. The performance at smaller power and smaller flow rate is the best of all.

As for yet another two ports configuration (d), it was not a very impressive performance.

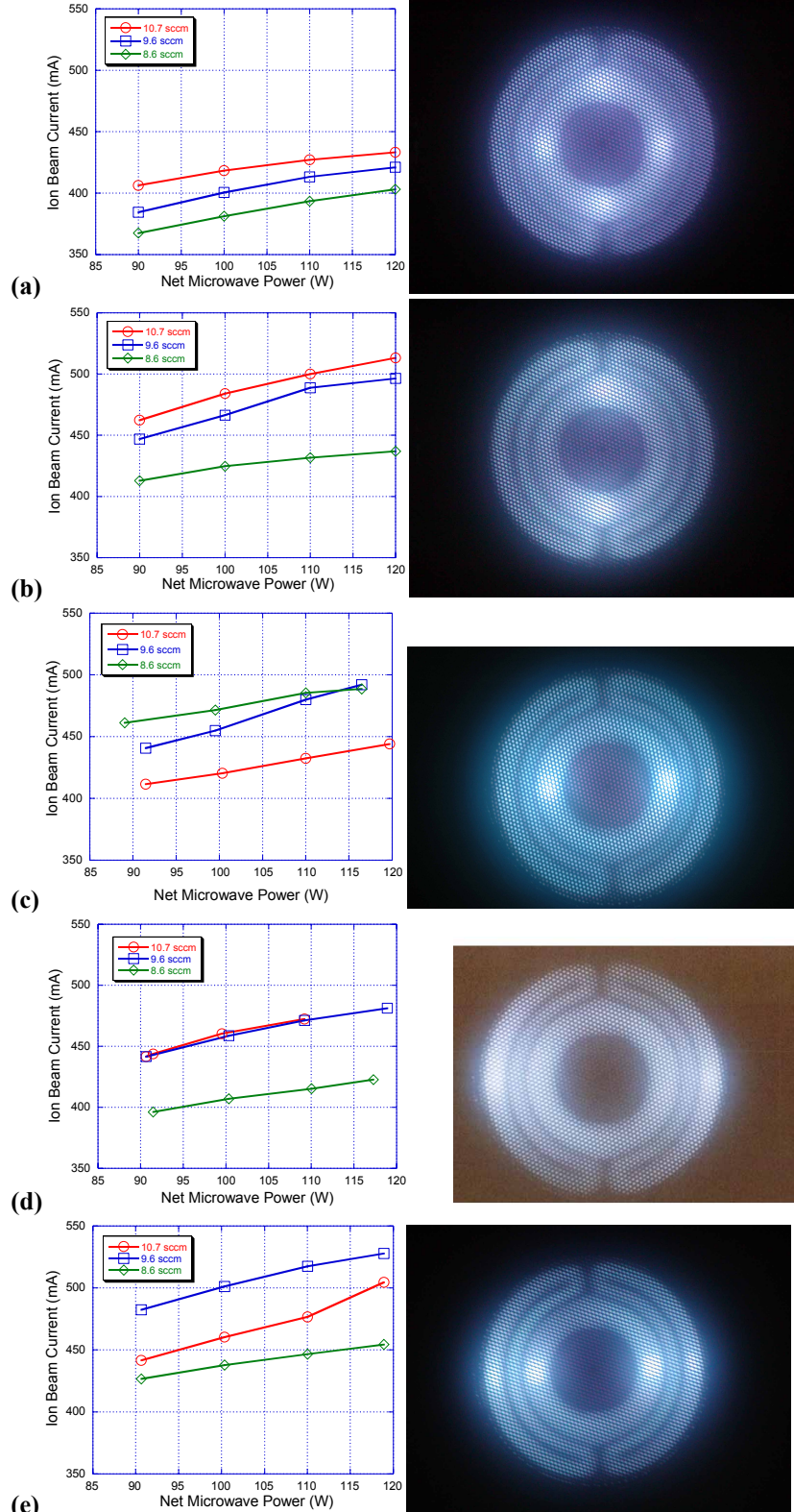


Figure 5. Ion beam current as a function of net microwave power. Two or four luminous spots in the right hand side pictures are the gas injection points on the end plate.

However, the configuration (e), which is combination of (c) and (d), achieved the best performance that has its peak at a flow rate of 9.6sccm. The ion beam current at the nominal operating power of 100W is as large as the target value of 500mA, and 25 % higher than that of the worst case (a).

Ion beam profile was measured with a 1mm-diameter tungsten probe located at 25mm downstream from the decelerator grid. The probe was traversed in radial direction so that it passes over the gas ports No.2 and No.6 by a stage with a stepping motor and the beam profile was measured. To repel electrons negative voltage $-30V$ was applied. Figure 6 shows the beam profiles for the cases (c)-(e). Small ripples in the current distributions are the effect of beamlets. In the case (c) current density peak is located inside the most inner magnet ring (1S in Figure 4) where the plasma confinement is weak due to the diverging magnetic field. Beam current produced in the outer magnets is very small. In the (d)-type configuration the beam profile is relatively flat but the outer most magnet rings produces still less ion beam. In the best case (e) the beam current distribution in the outer plasma region is flatter. The current density between magnet rows "3S" and "4N" is the highest of all the cases. Because the beam area of this outer most region occupies relatively large fraction of the total beam area, the current increase here contributes to the performance improvement.

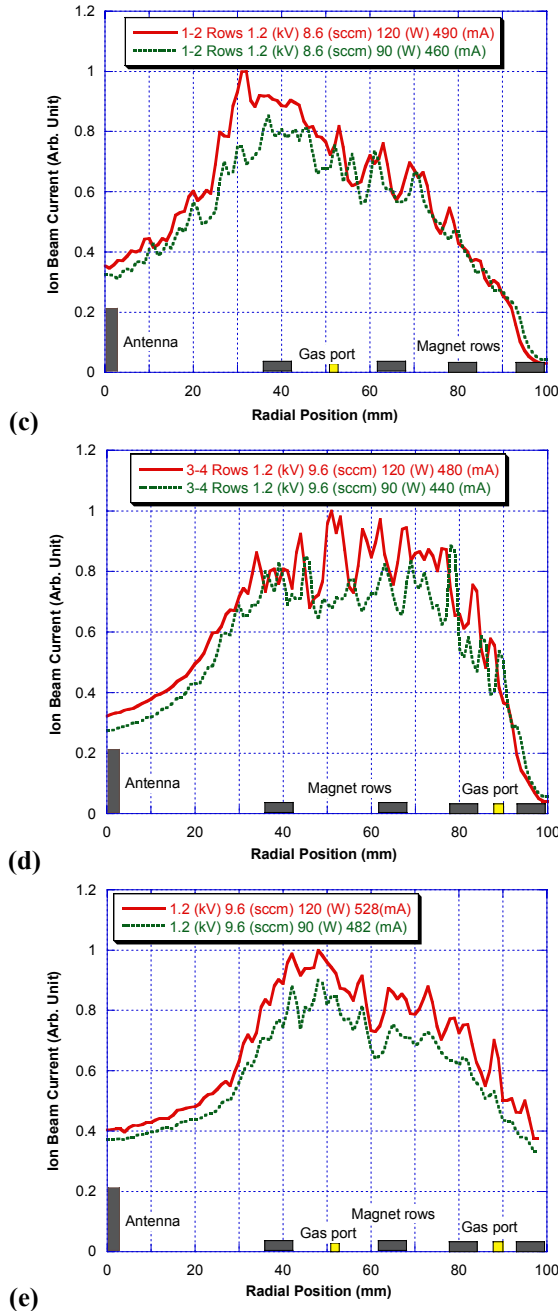


Figure 6. Ion beam current profiles for gas port configurations (c)-(e).

Although we do not fully understand the physics and design strategy concerning this theme, we can say that the optimization of propellant injection is very important and worth trying. For better understanding plasma diagnostics to clarify the electron heating process and plasma properties distribution overlaid to the microwave E-filed pattern would be required. The effect of propellant injection from the side wall of the discharge chamber has not been investigated yet. This is future work.

Figure 7 shows the performance curve of the best case (e). The peak values are ion production cost of 225W/A and propellant utilization of 72%, respectively. The future elimination of the reverse power 15W by some kind of impedance matching will lower the cost to the target value 200W/A. Closing the screen grid holes in the central region within 30mm in radius where the ion production rate is very low may improve the propellant utilization. This is also future work.

Figure 7 shows the performance curve of the best case (e). The peak values are ion production cost of 225W/A and propellant utilization of 72%, respectively. The future elimination of the reverse power 15W by some kind of impedance matching will lower the cost to the target value 200W/A. Closing the screen grid holes in the central region within 30mm in radius where the ion production rate is very low may improve the propellant utilization. This is also future work.

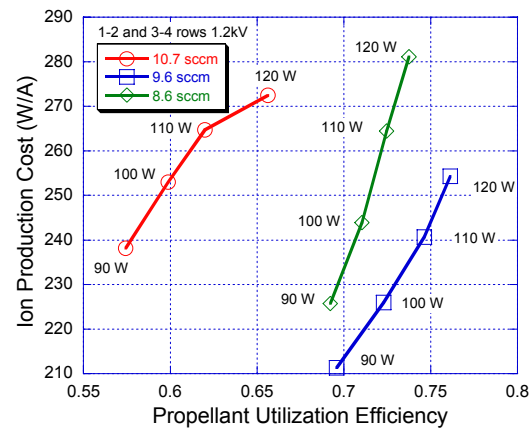


Figure 7. Performance curve obtained with the best propellant feed configuration.

III. Neutralizer

Enhancement of ion beam current on $\mu 20$ requests to scale up electron emission current from the microwave discharge neutralizer. The neutralizer designed same to the $\mu 10$ was devoted to the test to extract 500mA electron current with enhanced microwave power and mass flow rate. Large potential gap induces the sputtering erosion of the nozzle and the microwave feed probe. The previous paper¹⁰ insisted that a long life of the microwave discharge neutralizer over 10,000 hours is achieved at the contact voltage less than 50V, which is also an R&D target of the neutralizer for $\mu 20$. Optimization of the magnetic strength and the nozzle configuration reduced the contact voltage. Figure 8 shows the VI characteristics with constant mass flow rates. The contact voltage less than 50V at 500mA electron current is achieved at the mass flow rate over 0.5sccm and the microwave power 15W. If we consider the throttling of the ion engine system, not only the ion beam current but also the neutralizing electron current should be proportional to the mass flow rate in order to keep the specific impulse. In case to keep the ratio of electron current 500mA to mass flow 1sccm, the operational curve is represented by the red bold line in Figure 8. This device can neutralize the ion beam between 250mA and 600mA at less than 40V contact voltage. Figure 9 was taken at the first time combined operation of the ion source and the neutralizer of $\mu 20$. The neutralizer performance was confirmed to be almost the same as what was achieved in the diode configuration.

IV. Conclusion

The microwave discharge ion thruster $\mu 20$ is under development. Magnetic field and propellant injection method of the ion source has been optimized. The performance is highly dependent on the propellant injection method. Carbon-carbon optics passed the vibration test. Another thinner screen grid is to be evaluated to improve the thruster performance. The same neutralizer as $\mu 10$ can be used more efficiently with small addition of propellant and microwave power. The increase of propellant utilization efficiency by reducing the gas leak from the central region and decrease of ion production cost by reducing microwave reverse power are the future work.

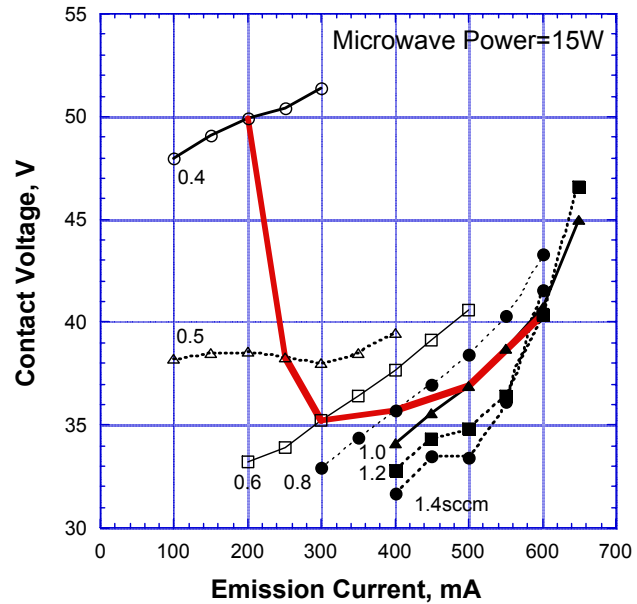


Figure 8. VI characteristics of neutralizer for $\mu 20$.

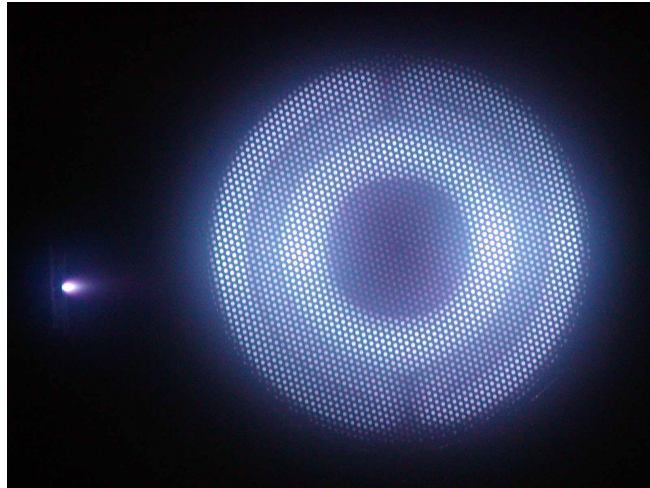


Figure 9. Combined operation of the ion source and the neutralizer of $\mu 20$.

References

¹Kuninaka, H. and Nishiyama, K., "Development of 20cm Diameter Microwave Discharge Ion Engine " $\mu 20$," *AIAA Joint Propulsion Conference*, AIAA-2003-5011, July 2003.

²Goede, H., “30-cm Electron Cyclotron Plasma Generator,” *Journal of Spacecraft*, Vol.24 No. 5, pp.437-443, September-October 1987.

³Miyoshi, H., Ichimura, S., Kuninaka, H., Kuriki, K., Horiuchi, Y., “Microwave Ion Thruster with Electron Cyclotron Resonance Discharge,” IEPC Paper 91-084, October 1991.

⁴Kuninaka, H., Hiroe, N., Kitaoka, K., Ishikawa, Y, Nishiyama, K and Horiuchi, Y., “Development of Ion Thruster System for Interplanetary Missions,” IEPC Paper 93-198, September 1993.

⁵Geisler, M., Kieser, J. and Wilhelm, R., “Elongated microwave electron cyclotron resonance heating plasma source,” *Journal of Vacuum and Science Technology A*, Vol. 8, No.2, pp.908-915, March-April 1990.

⁶Funaki, I., et al., “Verification Tests of 10-cm-diam. Carbon-Carbon Composite Grids for Microwave Discharge Ion Thruster,” IEPC Paper 99-164, October 1999.

⁷Nishiyama, K., Kuninaka, H., Shimizu, Y. and Toki, K. “30mN-class Microwave Discharge Ion Thruster”, IEPC Paper 2003-62, March 2003.

⁸Shimizu, Y., Kuninaka, H., Nishiyama, K. and Toki, K., “Evaluation of New Carbon-Carbon Composite Material for a 20 cm Ion Engine”, IEPC 2003-97, International Electric Propulsion Conference, Toulouse, March 2003.

⁹Toki, H., Fujita, H., Nishiyama, K., Kuninaka, H., Toki, K. and Funaki, I., “Performance Test of Various Discharge Chamber Configurations for ECR Discharge Ion Thruster,” IEPC Paper 01-107, October 2001.

¹⁰Kuninaka, H., Funaki, I., Nishiyama, K., Shimizu, Y. and Toki, K., “Result of 18,000-Hour Endurance Test on Microwave Discharge Ion Thruster Engineering Model”, *AIAA Joint Propulsion Conference*, AIAA 2000-3276, July 2000.